Analog Integr Circ Sig Process (2009) 59:53–64
DOI 10.1007/s10470-008-9238-x

Tunable frequency versatile filters implementation using minimum number of passive elements

Jinguang Jiang · Yigang He

Received: 5 July 2007 / Revised: 29 July 2008 / Accepted: 20 October 2008 / Published online: 27 November 2008

Abstract Two new universal active current-mode filters are proposed, one topology of which is with three inputs and one output, the other prototype is with single input and three outputs counterpart. One proposed circuit employs two current conveyors, two grounded capacitors and two resistors, wherever the other proposed circuit employs two current conveyors, two grounded capacitors and two multi-input, multi-output Operational Transconductance Amplifiers(OTA) as variable resistor for tuning the cutoff frequency of realized filters. Without changing the passive elements, the proposed circuits employ features of multi-functional, convenient for integration, low sensitivities and simple in structure.

Keywords Current-mode · Current conveyor (CCII) · Operational-Transconductance Amplifier (OTA) · Tunable frequency · Universal filter

1 Introduction

Current-mode universal filters employing current conveyors have been received considerable attentions. Due to their convenience and versatility in terms of signal processing for practical applications [1–43]. Also, a number of design of multiple-input single-output and single-input multiple-output current-mode and voltage-mode filters have been presented [18–27], universal filters are able to achieve more than one basic filter functions simultaneously with the same topology. A number of simultaneously versatile realized functions have been developed by a slight modification of the circuit. This is mainly attributable to the facility with which current outputs and current feedback can be developed when multiple current outputs are used.

Many CC-based voltage-mode universal biquadratic filters of three inputs and one output were proposed [4, 5, 20]. However, the circuit configurations in [5, 6] require too many current conveyors, for example, circuit proposed by H.Y. Wang [20] has three current conveyors. Compared with voltage-mode counterpart, current-mode universal filters are more attractive for their higher signal bandwidth, greater linearity and larger dynamic range. In the year 1991, C.M. Chang and P.C. Chen proposed a circuit configuration with one input and three outputs using seven current conveyors, grounded capacitors and resistors [4], In the year 2001, circuit proposed by H.Y. Wang and C.T. Lee [20] employs three current conveyors, two grounded capacitors and two resistors. These circuits can realize all the standard filter functions, namely, low-pass, band-pass, high-pass. Simultaneously, other functions of notch and all-pass can also be realized by properly connecting outputs without using additional active elements. However, many applications require filter tuning, in above cases, it is desirable to vary the filter coefficients electronically.

The major intention of this paper is to present new current-mode configurations, based on minimum number of grounded passive elements, current conveyors, Operational Transconductance Amplifiers. These circuits can simultaneously realize the five filter functions directly or indirectly. Firstly, a new current-mode three inputs and one output universal filter is proposed, which employs of two current conveyors and minimum number of passive

J. Jiang (✉)
GNSS Research Center, Wuhan University, Wuhan 430079, Hubei, China
e-mail: jgjiang95@yahoo.com.cn

Y. He
College of Electrical and Information Engineering, Hunan University, Changsha 410082, Hunan, China

elements of only two grounded capacitors and two resistors. The proposed circuit can realize low-pass, band-pass and high-pass filters all at high impedance outputs, and is very convenient for cascadability. Notch and all-pass functions can also be simply realized by connecting the appropriate output nodes. Secondly, another new current-mode low sensitivities one input and three outputs universal filter is also proposed, which uses of two current conveyors, one multi-inputs, multi-outputs OTA and minimum number of passive elements of two grounded capacitors. Through tuning the bias current value of OTA in order to change the gm value of OTA, a tunable cutoff frequency universal filter can be developed, which also possesses a low input impedance and high output impedance. The realization of a notch function does not require additional current conveyors, as such a realization can simply be achieved by connecting the appropriate node. Simulation results are given to illustrate the performances of the proposed circuits.

The paper is organized as follows. Section 2 presents two new universal filters based on multiple outputs second generation current conveyor(MOCCII) and multiple outputs OTA, the value of OTA can be tuned by changing its bias current, which makes these filters' cutoff frequency tunable. In Sect. 3, an automatic frequency tuning implementation using a switched-capacitor resistor and Operational Transconductance Amplifier is discussed. Section 4 contains simulations of universal current-mode filters, while Sect. 5 concludes the paper.

2 Circuit description

2.1 Basic building block of CCII ± and OTA

The practical terminal relations of MOCCII can be described as:

$$\begin{bmatrix} i_y \\ V_x \\ i_{z1} \\ \cdot \\ i_{zn} \\ i_{\bar{z}1} \\ \cdot \\ i_{\bar{z}n} \end{bmatrix} = \begin{bmatrix} 0 & 000 \\ \beta & 000 \\ 0 & \alpha 00 \\ \cdot & \cdots \\ 0 & \alpha 00 \\ 0 & (-\alpha)00 \\ \cdot & \cdots \\ 0 & (-\alpha)00 \end{bmatrix} \times \begin{bmatrix} V_y \\ i_x \\ V_z \\ Z_{\bar{z}} \end{bmatrix} \tag{1}$$

$$V_x = \beta V_y; i_z = \alpha i_x; i_{\bar{z}} = -\alpha i_x \tag{2}$$

From Fig. 1, Multiple outputs of z terminals of current conveyors can be developed employing current mirror technique.

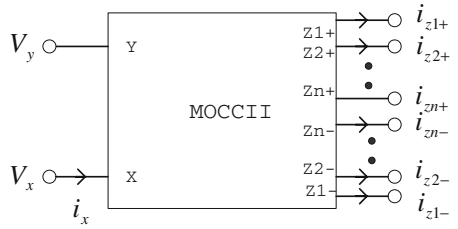

Fig. 1 Multiple outputs CCII (MOCCII)

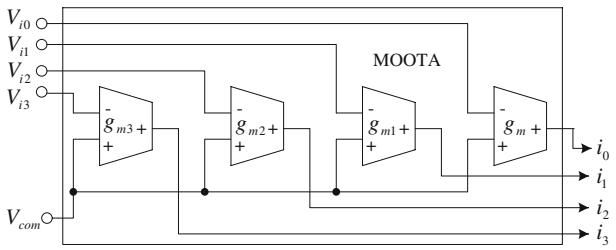

Fig. 2 Multiple outputs OTA (MOOTA)

From Fig. 2, The ideal terminal relations of multiple inputs and multiple outputs operational amplifier (MOOTA) can be described as:

$$i_0 = -g_m V_{i0} \quad i_1 = -g_{m1} V_{i1} \tag{3}$$

$$i_2 = -g_{m2} V_{i2} \quad i_3 = -g_{m3} V_{i3} \tag{4}$$

Taking the non-idealities of MOCCIIs into account, namely, $V_x = \beta V_y$, $\beta = 1 - \varepsilon_v$ ($\varepsilon_v << 1$) denotes the voltage tracking error of port y. $i_z = \alpha i_x$, $\alpha = 1 - \varepsilon_i (\varepsilon_i << 1)$ denotes the current tracking error of the port z. The first proposed three-input one-output filter is constructed with two current conveyors, and four grounded passive elements, as shown in Fig. 3.

If the two MOCCIIs are integrated in the same chip, the tracking error of each MOCCII is the same, that is:

$$\varepsilon_i^{(1)} = \varepsilon_i^{(2)} = \varepsilon_i, \ \varepsilon_v^{(1)} = \varepsilon_v^{(2)} = \varepsilon_v \tag{5}$$

For $\varepsilon << 1$, ignore high order items of equation, the output functions can be derived as:

$$\begin{aligned} I_0 &= \frac{I_{in1}s^2 - I_{in2}s\frac{1}{\alpha_2\beta_2 C_1 R_1} + I_{in3}\frac{1}{\alpha_2\beta_1\beta_2 C_1 C_2 R_1 R_2}}{s^2 + s\frac{1}{\alpha_2\beta_2 C_1 R_1} + \frac{1}{\alpha_1\alpha_2\beta_1\beta_2 C_1 C_2 R_1 R_2}} \\ &\approx \frac{s^2 I_{in1} - \frac{1}{(1-\varepsilon_i-\varepsilon_v)C_1 R_1} s I_{in2} + \frac{1}{(1-2\varepsilon_i-2\varepsilon_v)C_1 C_2 R_1 R_2} I_{in3}}{s^2 + \frac{1}{(1-\varepsilon_i-\varepsilon_v)C_1 R_1} s + \frac{1}{(1-2\varepsilon_i-2\varepsilon_v)C_1 C_2 R_1 R_2}} \end{aligned} \tag{6}$$

Compared with following equation:

$$I_0 \approx \frac{s^2 I_{in1} - \frac{\omega_0'}{Q'} s I_{in2} + \omega_0'^2 I_{in3}}{s^2 + \frac{\omega_0'}{Q'} s + \omega_0'^2} \tag{7}$$

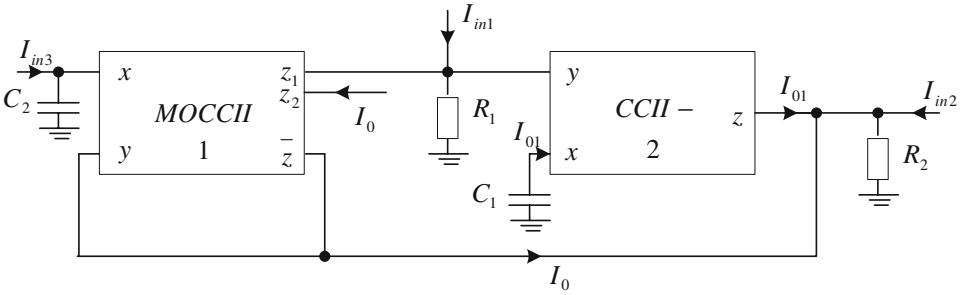

Fig. 3 The proposed current-mode three-input, one-output universal filter

$$\omega_0^{'} = \frac{1}{\sqrt{\alpha_1\alpha_2\beta_1\beta_2}}\omega_0 \approx \frac{1}{1-\varepsilon_i-\varepsilon_v}\omega_0 \tag{8}$$

$$Q^{'} = \sqrt{\frac{\alpha_2\beta_2}{\alpha_1\beta_1}}Q = Q \tag{9}$$

From (7), (8), (9), We can see that ε has little influence on parameter $\omega_0^{'}$ and no influence on $Q^{'}$.

The $\omega_0^{'}$ and $Q^{'}$ sensitivities of the filter are found as:

$$S_{R_1}^{\omega_0^{'}} = S_{R_2}^{\omega_0^{'}} = S_{C_1}^{\omega_0^{'}} = S_{C_2}^{\omega_0^{'}} = -\frac{1}{2} \tag{10}$$

$$S_{C_1}^{Q^{'}} = S_{R_1}^{Q^{'}} = \frac{1}{2},\ S_{C_2}^{Q^{'}} = S_{R_2}^{Q^{'}} = -\frac{1}{2} \tag{11}$$

Which are no more than one in magnitude.

Moreover, the configuration in Fig. 4 can function as a single-input, three-output universal filter if and by taking as the single input terminal. From (7), the current transfer functions can be derived as low-pass, band-pass and high-pass responses, respectively, when

$$\frac{I_{HP}}{I_{in}} = -\frac{s^2}{A(s)} \tag{12}$$

$$\frac{I_{BP}}{I_{in}} = \frac{\frac{g_{m2}}{C_1}s}{A(s)} \tag{13}$$

$$\frac{I_{LP}}{I_{in}} = -\frac{\frac{g_m g_{m2}}{C_1C_2}}{A(s)} \tag{14}$$

$$\frac{I_{NH}}{I_{in}} = -\frac{s^2+\frac{g_{m1}g_{m2}}{C_1C_2}}{A(s)} \tag{15}$$

$$\frac{I_{AP}}{I_{in}} = \frac{s^2 - s\frac{g_{m3}}{C_1} + \frac{g_{m1}g_{m2}}{C_1C_2}}{A(s)} \tag{16}$$

$$A(s) = s^2 + s\frac{g_{m3}}{C_1} + \frac{g_{m1}g_{m2}}{C_1C_2} \tag{17}$$

$$\omega_0 = \sqrt{\frac{g_{m1}g_{m2}}{C_1C_2}}\ Q = \frac{1}{g_{m3}}\sqrt{\frac{C_1}{C_2}g_{m1}g_{m2}} \tag{18}$$

The $\omega_0^{'}$ and $Q^{'}$ sensitivities of the filter are found as:

$$S_{g_m}^{\omega_0} = 0,\ S_{g_{m3}}^{\omega_0} = 0,\ S_{g_{m1}}^{\omega_0} = S_{g_{m2}}^{\omega_0} = \frac{1}{2},\quad S_{C_1}^{\omega_0} = S_{C_2}^{\omega_0} = -\frac{1}{2} \tag{19}$$

$$S_{g_m}^{Q} = 0,\ S_{g_{m3}}^{Q} = -1,\ S_{g_{m1}}^{Q} = S_{g_{m2}}^{Q} = \frac{1}{2} \tag{20}$$

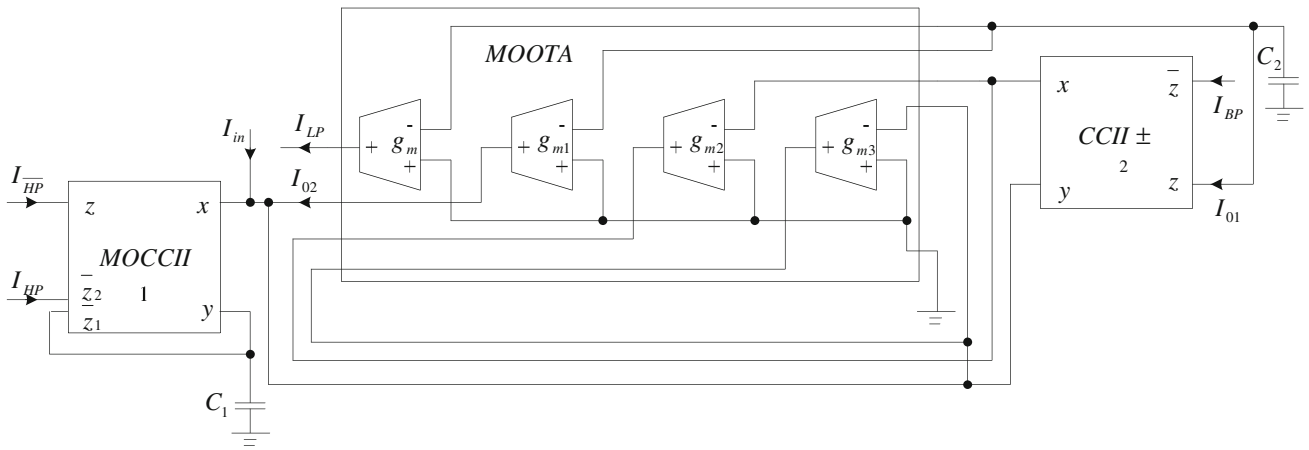

Fig. 4 The proposed current-mode single-input, three-output universal filter

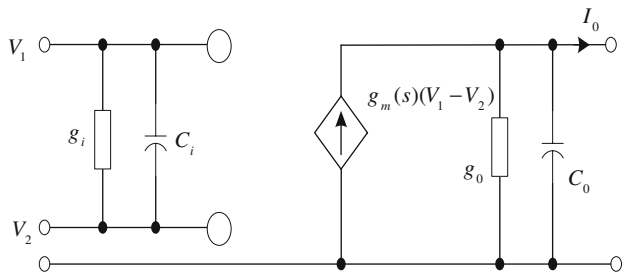

Fig. 5 Practical OTA macro-model

$$S_{C_1}^{Q} = \frac{1}{2},\ S_{C_2}^{Q} = -\frac{1}{2} \tag{21}$$

Which are also no more than one in magnitude.

We can now discuss practical problems in design of filters employing OTA and MOCCII. In particular we will deal with the effects of OTA nonidealities on filter performance. The methods for the evaluation and reduction of effects will be proposed as follows.

An OTA macro-model with finite input and output impedances and transconductance frequency dependence is shown in Fig. 5. We use g_i and C_i to represent the differential input conductance and capacitance and drop subscript d (for differential) for simplicity. g_0 and C_0 are those at the output. The common-mode input conductance g_{ic} and capacitance C_{ic} are ignored because they are usually very small in practice compared with differential counterparts and can be absorbed as many filter structures have a grounded capacitor or a grounded OTA resistor from OTA input terminals to ground.

$$\alpha_1 = \alpha_2 = \alpha;\ \beta_1 = \beta_2 = \beta \tag{22}$$

$$Y_i = g_i + sC_i\ Y_0 = g_0 + sC_0 \tag{23}$$

$$C_{i0} = C_{i1} = C_{i2} = C_{i3} = C_i$$

$$g_{i0} = g_{i1} = g_{i2} = g_{i3} = g_i \tag{24}$$

$$C_{00} = C_{01} = C_{02} = C_{03} = C_0$$

$$g_{00} = g_{01} = g_{02} = g_{03} = g_0 \tag{25}$$

$$\frac{I'_{HP}}{I_{in}} = \frac{N_{HP}(s)}{D_n(s)} \tag{26}$$

$$\frac{I'_{BP}}{I_{in}} = \frac{N_{BP}(s)}{D_n(s)} \tag{27}$$

$$\frac{I'_{LP}}{I_{in}} = \frac{N_{LP}(s)}{D_n(s)} \tag{28}$$

$$\begin{aligned} D_n(s) = {} & s^2(C_2 + C_i)[(C_1 + \alpha\beta(2C_0 + C_i)] \\ & + \{\alpha\beta[(C_0 + C_i)(g_i + \alpha\beta g_{m1}) \\ & + (C_2 + C_i)(g_{m3} + 2g_0 + g_i)] + g_i(C_1 + \alpha\beta C_0)\}s \\ & + \alpha\beta[g_i(g_{m3} + 2g_0 + g_i) + \alpha\beta g_{m1}(g_{m2} + g_0 + g_i)] \end{aligned} \tag{29}$$

$$N_{HP}(s) = -s\alpha C_1[g_i + s(C_2 + C_i)] \tag{30}$$

$$N_{BP}(s) = \alpha^2\beta^2[g_{m2} + g_0 + g_i + s(C_0 + C_i)][g_i + s(C_2 + C_i)] \tag{31}$$

$$N_{LP}(s) = -\alpha^2\beta^2 g_m[g_{m2} + g_0 + g_i + s(C_0 + C_i)] \tag{32}$$

$$\omega_0' = \left\{\frac{\alpha\beta[g_i(g_{m3} + 2g_0 + g_i) + \alpha\beta g_{m1}(g_{m2} + g_0 + g_i)]}{(C_2 + C_i)[C_1 + \alpha\beta(2C_0 + C_i)]}\right\}^{1/2} \tag{33}$$

$$Q' = \frac{\left\{\frac{\alpha\beta[g_i(g_{m3}+2g_0+g_i)+\alpha\beta g_{m1}(g_{m2}+g_0+g_i)]}{(C_2+C_i)[C_1+\alpha\beta(2C_0+C_i)]}\right\}^{1/2}}{\alpha\beta[(C_0 + C_i)(g_i + \alpha\beta g_{m1}) + (C_2 + C_i)(g_{m3} + 2g_0 + g_i)] + g_i(C_1 + \alpha\beta C_0)} \tag{34}$$

It can be seen that the low-pass frequency responses of filter are little influenced by nonideal factors of OTA, the higher frequency, the higher influence.

The CMOS realization of MOCCII is shown in Fig. 6. However, it is possible to represent an MOCCII using Operational Amplifier (OA) and a small-signal current mirror as shown in Fig. 7.

The proposed circuit implementation of multiple inputs and multiple outputs OTAs are shown in Fig. 2 if input and output conductances of non-idealities of OTAs are taken into account, the input and output immittances can be written as (23). The CMOS implementation of single g_m cell of MOOTA is shown in Fig. 8.

3 Automatic frequency tuning by switched capacitor and Operational Transconductance Amplifier (OTA)

A fully differential tuning circuit is used to generate the control voltages V_{C+} and V_{C-} [28–40]. The tuning circuit is

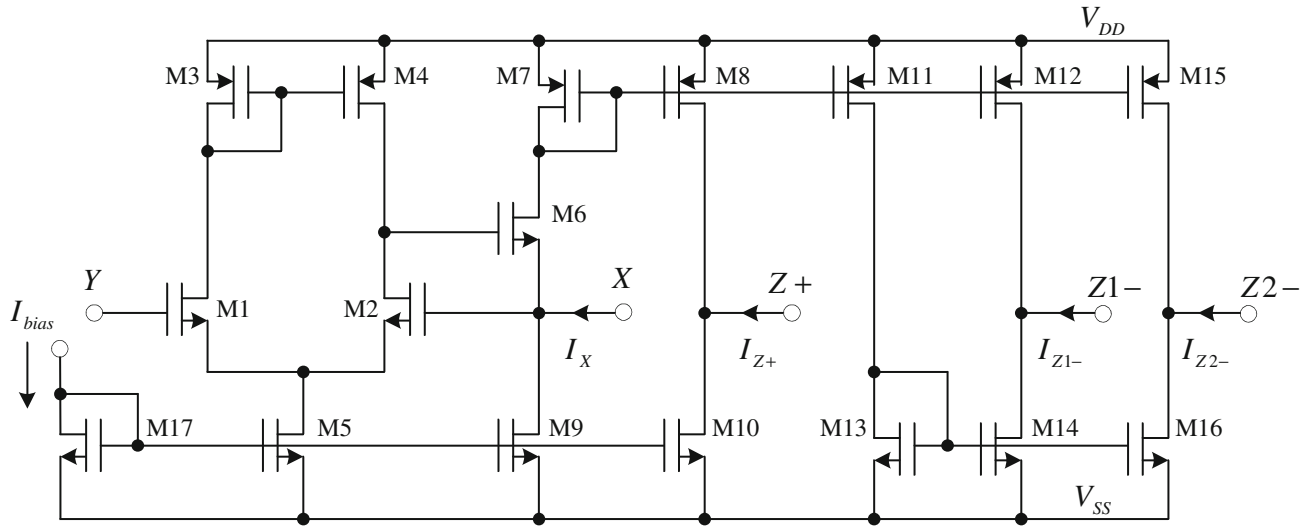

Fig. 6 CMOS implementation of MOCCII

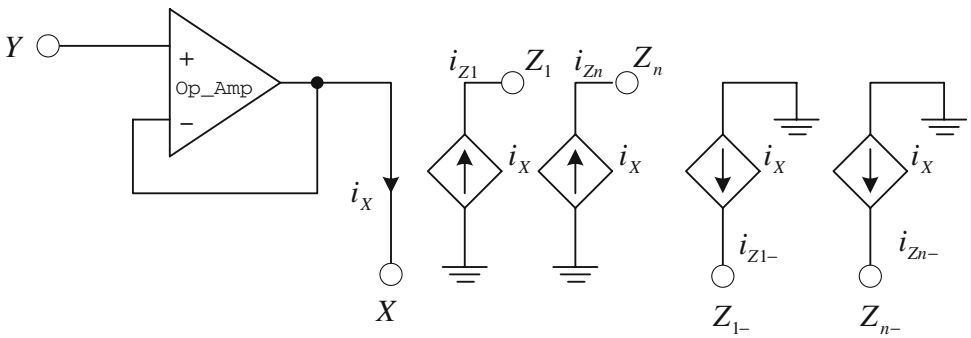

Fig. 7 Implementation of an ideal MOCCII

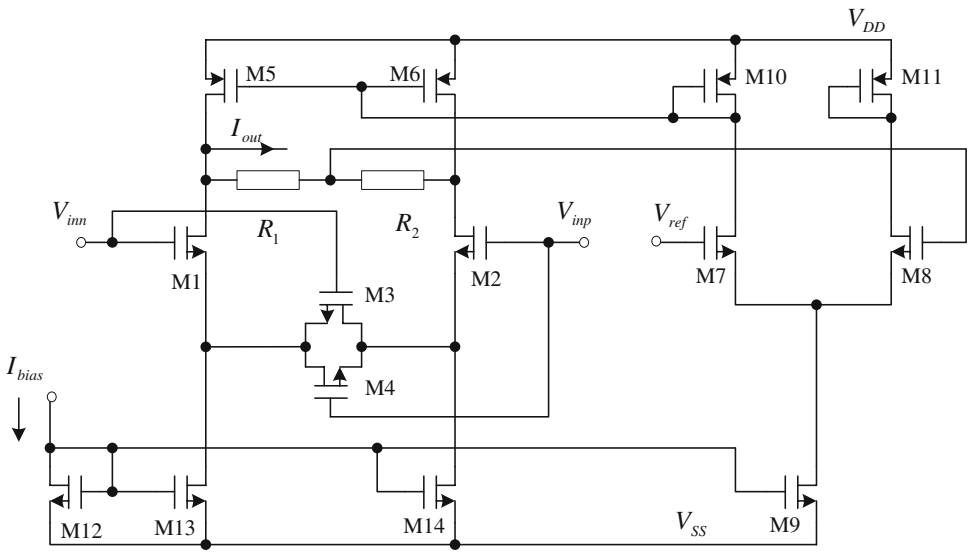

Fig. 8 CMOS implementation of single g_m cell of Multiple Outputs OTA (MOOTA) in Fig. 2

designed to allow tuning of the filter's cutoff frequency and minimize the influence of the process parameters and operating conditions. Since the active filter's frequency characteristic is determined by g_m value of MOOTA, C_1 and C_2, any process variation and temperature dependencies can be compensated by tuning the g_m value of the MOOTA. As explained above, the value of g_m can be tuned by bias current which is determined by controlling the gate voltages of current mirrors of transistors M12 and M13 in Fig. 8. The required control voltages V_{C+} and V_{C-} are generated in the

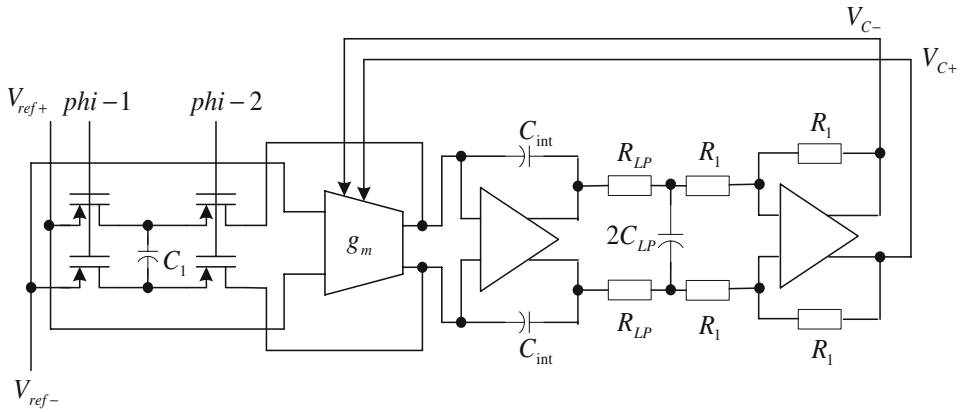

Fig. 9 Automatic frequency tuning circuit

tuning circuit shown in Fig. 9, which is based on the balancing principle that a switched-capacitor network is accurately to implement a reference time constant, which depends solely on capacitor matching. Shown in the left portion of the schematic Fig. 9 is the time-constant matching integrator of the continuous-time equivalent resistor path and the switched-capacitor equivalent resistor path. The time constant of the continuous-time equivalent resistor path is C_{int}/g_m, and that of the switched-capacitor equivalent resistor patch is $C_{\text{int}}/(f_{clk}C_1)$. The mismatch of the two time constants, which simplifies as the mismatch of equivalent resistors $1/g_m$ and $1/(f_{clk}C_1)$, is reflected at the output of the integrator. That voltage is then translated to the control voltage of the MOOTA. Equilibrium is reached when $g_m = f_{clk}C_1$. The right portion of the schematic is the g_m value controlling voltage generating circuit of MOOTA.

At each of the integrator inputs, two currents, $I_{g_m}$and I_{SC} are summed. The currents flow from the reference voltages, V_{ref+} and V_{ref-}, to the integrator inputs, which are at virtually the same potential as analog ground. The positive and negative reference voltages are symmetrical around analog ground. I_{SC} is the current through the switched capacitor resistor realization R_{SC}, while I_{g_m} is the current through transconductor structure. The transconductor is identical to the ones used in the filter and controlled by the same voltages V_{C+} and V_{C-}. These control voltages are fed back from the outputs of the tuning circuit to the transconductor structure and control its equivalent transconductor g_m in such a way that $I_{SC} = I_{g_m}$ in steady state condition. Equilibrium is reached when $g_m = f_{clk}C_1$. The output voltage of the integrator is symmetrical around a constant common voltage, $V_{\text{common}} = V_{DD}/2$, and therefore V_{C+} and V_{C-} are symmetrical around a constant $\bar{V}_C$.

In order to tune the cutoff frequency of the filter, the resistance implemented by the switched-capacitor circuit, $R_{SC} = 1/(f_{clk}C_1)$, can be changed by using a variable clock frequency. The integrator will then adjust the control voltages V_{C+} and V_{C-} until the equilibrium of the tuning circuit is reached again.

The unity-gain frequency of an integrator can be written as:

$$\omega_{\text{unity}} = \frac{g_m}{C_{\text{int}}} \tag{35}$$

In the tuning circuit, the equivalent resistance of transconductor and the one implemented by the switched-capacitor are equal in steady–state:

$$R_{eq} = \frac{1}{f_{clk}C_1} \tag{36}$$

Using above Eqs. 35 and 36, the equation for the unity-gain frequency can be rewritten as:

$$\omega_{\text{unity}} = f_{clk}\frac{C_1}{C_{\text{int}}} \tag{37}$$

Shown as above Eq. 37, mismatch in capacitors C_1 and C_{int}directly introduce frequency deviation of ω_{unity} of integrator which is proportional to ratio of C_1/C_{int}, assuming ideal matching between the components of the filter and the tuning circuit, the unity-frequency ω_{unity} is accurately set to $(f_{clk}C_1/C_{\text{int}})$, and hence precise frequency tuning can be achieved without any external components. Among the fabricated filter in Fig. 4, the ω_{unity} standard deviation is 5%, measured under a fixed capacitor, C_1, and the same reference frequency, f_{clk}. If a greater accuracy of the corner frequency is desired, a fine adjustment can be provided by means of either digitally trimming the capacitor C_1 or varying the clock frequency f_{clk}. The fine tuning of capacitor of C_1 for the corner frequency of the proposed filter in Fig. 4 can be accomplished within a $\pm 1\%$ absolute accuracy. Note that an additional low-pass filter, $R_{LP}C_{LP}$, has been added here to remove the high-frequency ripple voltage due to using a switched-capacitor circuit. It should also be noted that, since this method requires a clock signal, there is a strong possibility that some of the clock signal will leak into the continuous-time filter, either mainly through the Operational Transconductance Amplifier controlling signal, differential operational amplifier of Fig. 9 or through the IC substrate, in the mean time, since

the stability of the tuning voltage can be solved through placing a dominant pole in the control loop by choosing the product R_{LP} C_{LP} very large (alternately a large C_{int} can be used), a stable dc control voltage without ac ripple voltage is established. Any mismatch between the equivalent g_m cell resistor and switched-capacitor equivalent resistor causes current to flow into the integrator, which changes the control voltage V_{C+} and V_{C-}. The negative feedback loop controls the frequency of clock and adjusts the g_m cell equivalent resistor forcing it to be equal to the average resistance of the SC branch. Once the feedback loop reaches equilibrium, the two equivalent resistances will be equal. The tuning action applies equally to the tuning of the continuous-time filter employing MOCCII and OTA.

4 Simulation results

Universal filters are simulated using schematics of MOCCII and Operational Transconductor Amplifier implementation as depicted in Figs. 3 and 4. All MOS transistors are operated in saturation region and all of the bulks are connected to the sources. The simulations are performed using SPICE based on 0.35 μm Chartered CMOS process model parameters (PMOS_3p3, $V_{THP} = -0.837$ V, $\mu_P = 277$ cm^2/V s, $T_{OX} = 8.69$ nm), (NMOS_3p3, $V_{THN} = 0.6053$ V, $\mu_N = 413.7172$ cm^2/V s, $T_{OX} = 7.69$ nm). The MOCCII is constructed using the schematic implementation in Fig. 6 with dc supply voltages equal to 3.3 V and 0 V and bias current of transistor M17 is 10 μA, similarly the supply voltage of single OTA is the same as that of MOCCII, and bias current of transistor M12 in Fig. 8 is 20 uA. The dimensions of the MOS transistors used in MOCCII (shown in Fig. 6) and Operational Transconductance Amplifier (shown in Fig. 8)'s implementations are given in Table 1, 2.

To investigate what is the frequency for the designed MOCCII, AC simulations have been performed. The frequency responses of i_z/i_x, and V_x/V_y for MOCCII are depicted in Figs. 10 and 11. The frequency behavior reported in Fig. 12 suggests that for high frequency applications (frequencies of more than 90 MHz), a compensation is needed. The DC transfer characteristic of MOCCII is shown in Fig. 11.

The characteristic of input voltage Vin and output current I_{out} of OTA is shown in Fig. 13, when the supply

Table 1 Dimensions of CMOS transistors of MOCCII

PMOS transistors	W(μm)/L(μm)
M_3, M_4, M_7, M_8, M_{11}, M_{12} and M_{15}	30*2/2
NMOS transistors	W(μm)/L(μm)
M_1, M_2, M_5, M_6, M_9, M_{10}, M_{13}, M_{14} M_{16} and M_{17}	30/2

Table 2 Dimensions of CMOS transistors of Operational Transconductance Amplifier of Fig. 8

NMOS transistors	W(μm)/L(μm)
M_1, M_2	10*4/2.5
M_3, M_4	8*2/1
M_7, M_8	8/1
M_9	6*6/2
M_{12}, M_{13}, M_{14}	6*18/1
PMOS transistors W(μm)/L(μm)	
M_5, M_6,	6*18/2
M_{10}, M_{11}	6*4/2
Resistors (Ω)	
R_1, R_2	200 K

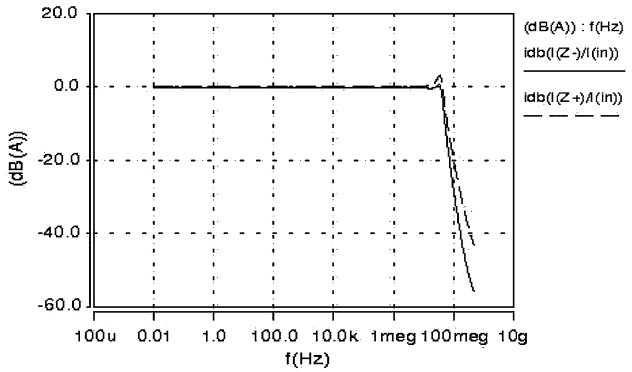

Fig. 10 The simulated frequency response of i_z/i_x for the MOCCII ($V_{DD} = 3.3$ V, $V_{SS} = 0$ V, $I_{bias} = 10$ uA)

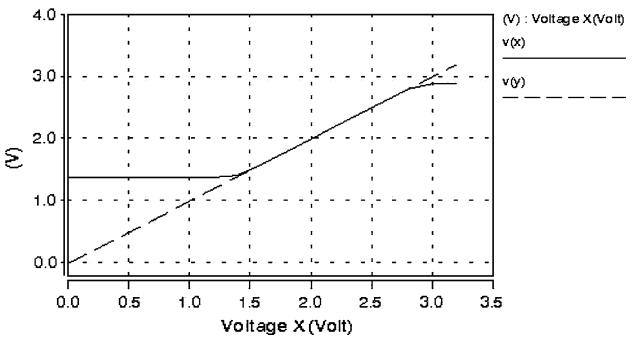

Fig. 11 $V_x - V_y$ DC transfer characteristic of MOCCII($V_{DD} = 3.3$ V, $V_{SS} = 0$ V, $I_{bias} = 10$ uA)

voltages used for OTAs of Fig. 8 are 3.3 V and 0 V, the bias currents of transistor M12 are selected as $I_{bias} = 20$ uA, It can be seen that gm value of OTA is 0.05174 mS.

To verify the theoretical analyses, active and passive bandpass responses of three-input, single-output filter are shown in Fig. 14. We selected the following setting to obtain the lowpass, bandpass and highpass responses in Fig. 3, with cutoff frequency of $f_0 = 15.92$ kHz, and a pole-quality factor of $Q = 1$: $R_1 = R_2 = 100$ K, $C_1 = C_2 = 100$ pf (circuit A); $Q = 2$: $R_1 = R_2 = 200$ K, $C_1 = 100$ pf,

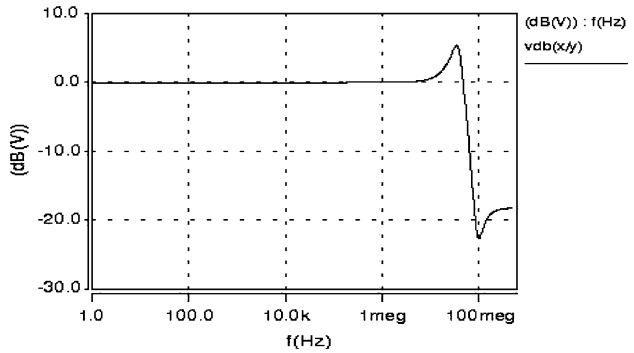

Fig. 12 The simulated frequency response of V_x/V_y for the MOC-CII($V_{DD} = 3.3$ V, $V_{SS} = 0$ V, $I_{bias} = 10$ uA)

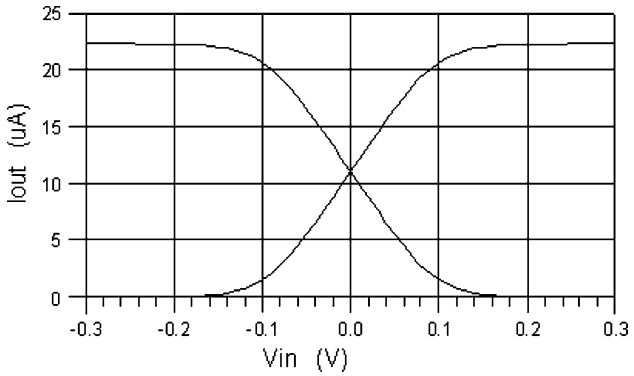

Fig. 13 Characteristic of input voltage Vin and output current Iout of Operational Transconductance Amplifier (OTA) ($V_{DD} = 3.3$ V, $V_{SS} = 0$ V, $I_{bias} = 20$ uA, $g_m = 0.05174$ mS)

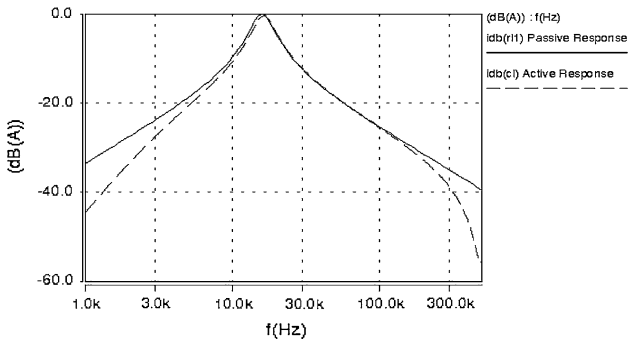

Fig. 14 Active and passive band-pass responses of three-input, single-output filter of Fig. 3

$C_2 = 25$ pf (circuit B); $Q = 3$: $R_1 = R_2 = 300$ K, $C_1 = 100$ pf, $C_2 = 11.11$ pf (circuit C); In the circuit of Fig. 3, the simulated values of f_0 and Q are 16 kHz and 1 for circuit A, 16 kHz and 2 for circuit B, and 16 kHz and 3 for circuit C, respectively. Figure 16 shows the responses for the lowpass, bandpass and highpass functions of the three-input single-output filter. All the results are in good agreement with the theoretical predictions.

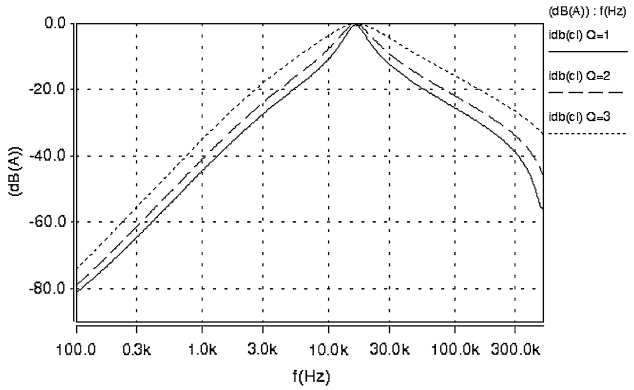

Fig. 15 Active band-pass responses of three-input, single-output filter of Fig. 3 in different quality factors

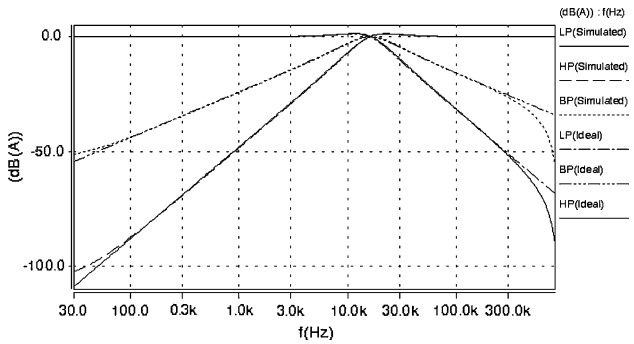

Fig. 16 Frequency responses of the three-input, single-output universal filter of Fig. 3 employs MOCCII and CCII-

Also the second-order current-mode filter of Fig. 4 is simulated. The active elements and biasing currents of MOCCII and MOOTA have been selected as $g_m = g_{m1} = g_{m2} = g_{m3} = 0.05174$ mS, $C_1 = C_2 = 100$ pf, I_{bias} (MOCCII) $= 20$ uA, I_{bias} (MOOTA) $= 20$ uA to obtain unity gain low-pass, band-pass, and high-pass responses with a natural pole frequency of $f_0 = 82.38$ kHz. The frequency responses of single-input, three-output universal filter with tunable frequency are shown in Fig. 17. When it functions as low-pass, band-pass and high-pass modes. The simulated results for MOCCII and OTA based single-input three-output universal filter of Fig. 4 are shown in Fig. 15. Employing above automatic frequency tuning technique by switched capacitor and Operational Transconductance Amplifier, and through adjusting the clock frequency of switched-capacitor, the cutoff frequency of single-input three-output universal filter can be tuned from 10 kHz to 300 kHz conveniently (Fig. 17). As shown in Fig. 17, the results also confirm the theoretical ones.

The transient responses of the three-input, one-output and single-input, three-output universal filters are shown in Figs. 18 and 19, respectively. Also, the large signal behavior of these two circuits in Figs. 3 and 4 are tested with investigation of the dependence of the output

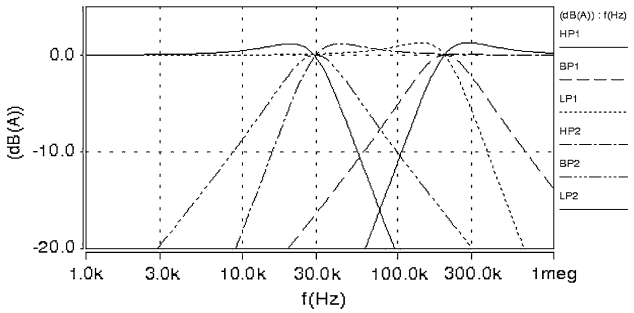

Fig. 17 Responses of the single-input, three-output filter of Fig. 4 employs MOCCII and OTA with tunable frequency

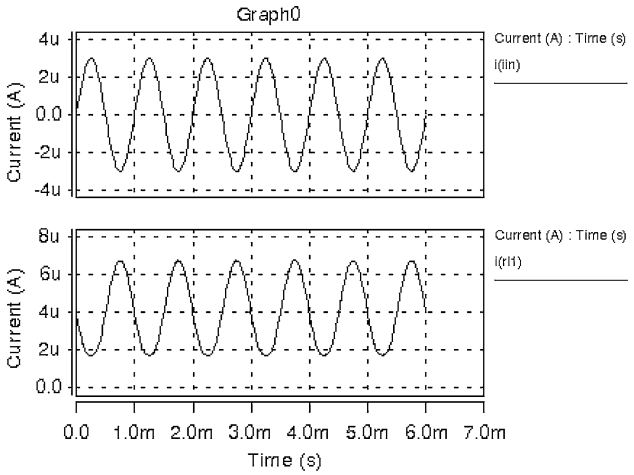

Fig. 18 Simulated transient responses of the three-input, one-output universal filter (the bias currents I_{bias} of MOCCII and CCII- are 20 uA, respectively, I_{in} is 3 uA, THD value of I_{rl1} is 6.2657%)

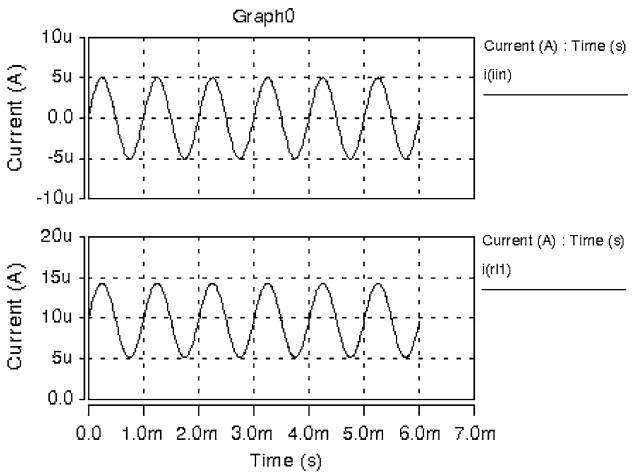

Fig. 19 Simulated transient responses of the single-input, three-output universal filter(the bias currents I_{bias} of MOCCII and MO are 20 uA, respectively, I_{in} is 5 uA, THD value of I_{rl1} is 1.1161%)

harmonic distortion for the low-pass response on the amplitude of the sinusoidal input signals at 1 kHz. The obtained THD simulation results for above two configurations in Figs. 3 and 4 are given in Tables 3 and 4, respectively. From Table 3, it can be seen that the harmonic distortion rapidly increases for the input current signal amplitude is beyond 3 uA, because much more larger input signal will result MOS transistors of MOCCII operating in triode region, when the bias currents of MOCCII and CCII- are 20 uA, respectively. whereas, Table 4 shows that larger input current signal amplitude results in higher value of THD due to the open-loop nature of MOOTA in single-input, three-output configuration. generally, the input voltage signal range of MOOTA should be smaller than 100 mV or so, which can also be seen from Fig. 13.

Since output currents of MOCCII are composed of multiple current mirrors, process mismatches between the current mirror transistors of MOCCII could be analyzed to determine the effects of THD on proposed universal filters. First, the current distortion caused by only threshold voltage mismatches of current mirrors is considered with $\Delta V_t = V_{t1} - V_{t2}$. Assume transistors of current mirror are identical except for the threshold voltage mismatch. The

Table 3 Dependence of output harmonic distortion of three-input, one-output filter of Fig. 3 on input current signal amplitude

Current amplitude (μA)	Total harmonic distortion (%)
0.1	0.0692
0.5	0.3516
1	0.7434
1.5	1.2457
2	2.0507
2.5	3.6635
3	6.2657
3.5	9.1141
4	11.7374
4.5	14.0387
5	16.0384

Table 4 Dependence of output harmonic distortion of single-input, three-output filter of Fig. 4 on input current signal amplitude

Current amplitude (μA)	Total harmonic distortion (%)
0.1	0.0223073
0.5	0.0269169
1	0.0595809
1.5	0.1053602
2	0.16992125
2.5	0.2544952
3	0.3608672
5	1.1161
6	3.8886
7	8.1568
8	11.8194

output current i_{out} is ideally identical to the signal current i, shown in (38). The expression for the output current with threshold voltage mismatch is:

$$i_{out} = i + \frac{2\Delta V_t I}{(V_{GS1} - V_{t1})}\sqrt{\left(1 + \frac{i}{I}\right)} + \frac{\beta}{2}\Delta V_t^2 \tag{38}$$

$$i_{out,dc} = \frac{\beta}{2}\Delta V_t^2 + \frac{2\Delta V_t I}{(V_{GS1} - V_{t1})} \tag{39}$$

Where $\beta = k'(W/L)$

$$i_{out,ac} = i\left[1 + \frac{\Delta V_t}{(V_{GS1} - V_{t1})}\right] + \frac{2\Delta V_t I}{(V_{GS1} - V_{t1})} \cdot \left[-\frac{1}{8}\left(\frac{i}{I}\right)^2 + \frac{1}{16}\left(\frac{i}{I}\right)^3 - \frac{5}{128}\left(\frac{i}{I}\right)^4 + \cdots\right] \tag{40}$$

Where i is the peak signal current. It is seen from (39) (40) that threshold voltage mismatch in the current-mirror transistors distorts the output current. The current is separated into a dc term in (39) and an ac polynomial term in (40). The dc offset shifts the bias point as indicated by $i_{out,dc}$ term in (39). The magnitude of ac gain error and harmonic distortion are determined by the first and second $i_{out,ac}$ terms, respectively. The harmonic distortion is a strong function of the peak signal-to-bias-current ratio i/I, and therefore, harmonic distortion is minimized by reducing the i/I ratio. Which is also the explanation that the simulated results of proposed filters (Figs. 3 and 4) have THD characteristics of monotonicity according to the amplitude of current input signals (0.1–5 u) when the bias currents of MOCCII, CCII- and MOOTA are 20 uA, respectively.

5 Conclusions

Versatile multi-input multi-output current-mode biquad configurations are introduced in this paper. The proposed universal filters has been exhibited by application on the implementation of three-input, single-output and single-input, three-output filters, which realize low-pass, high-pass, and band-pass responses. In addition, by changing the bias current of OTA through technique of switched capacitor, a tunable frequency single-input three-output universal filter construction has been obtained. Only two current conveyors and several grounded passive elements are necessary in both proposed filters. The proposed circuits enjoy the following features: (1) using minimum number of passive elements; (2) employing only grounded capacitors and resistors, which is convenient for monolithic integration; (3) frequency tunability; (4) high impedance outputs enable easy cascading in current-mode operation; (5) low sensitivity and simple in structure. The simulation results, which confirm the theoretical analysis, are given.

Acknowledgments The authors would like to thank China Postdoctoral Science Foundation, The National High Technology Research and Development Program of China (No. 2007AA12Z332), Doctoral Discipline Special Fund of Colleges and Universities of China for the financial support.

References

1. Sedra, A., & Smith, K. C. (1970). A second generation current conveyor and its application. *IEEE Transactions on Circuit Theory, CT-17*, 132–134.
2. Pal, K. (1989). Modified current conveyors and their applications. *Microelectronics Journal, 20*(14), 37–40. doi:10.1016/0026-2692(89)90076-1.
3. Wu, J., & Marsy, E. E. (1996). Current-mode ladder filters using multiple output current conveyors. *IEEE Proceedings Circuits, Devices ,and Systems, 143*(4), 218–222. Aug.
4. Chang, C. M., & Chen, P. C. (1991). Universal active current filter with three inputs and one output using current conveyors. *International Journal of Electronics, 71*(5), 817–819. doi:10.1080/00207219108925525.
5. Chang, C. M., & Lee, M. S. (1994). Universal voltage-mode filter with three inputs and one output using three current conveyors and one voltage follower. *Electronics Letters, 30*(25), 2110–2113. doi:10.1049/el:19941463.
6. Horng, J. W., Lee, M. H., Cheng, H. C., et al. (1997). Universal active current filter using two multiple current output OTAs and one CCIII. *International Journal of Electronics, 82*(3), 241–247. doi:10.1080/002072197136066.
7. Minaei, S., & Turkoz, S. (2004). Current-mode electronically tunable universal filter using only plus-type current controlled conveyors and grounded capacitors. *Etri Journal, 26*(4), 292–296. Aug.
8. Shaker, M. O., Mahmoud, S. A., et al. (2006). New CMOS fully-differential transconductor and application to a fully-differential Gm-C filter. *Etri Journal, 28*(2), 175–181.
9. Yuce, E., Cicekoglu, O., et al. (2006). CCII-based grounded to floating immittance converter and a floating inductance simulator. *Analog Integrated Circuits and Signal Processing, 46*(3), 287–291. doi:10.1007/s10470-006-1624-7.
10. Yuce, E., Minaei, S., & Cicekoglu, O. (2005). A novel grounded inductor realization using a minimum number of active and passive components. *Etri Journal, 27*(4), 427–432.
11. Jiang, J., & Wang, Y. (2006). Design of a tunable frequency CMOS fully differential fourth-order Chebyshev filter. *Microelectronics Journal, 37*(1), 84–90. doi:10.1016/j.mejo.2005.06.017.
12. Mahmoud, S. A. (2006). New fully-differential CMOS second-generation current conveyor. *Etri Journal, 28*(4), 495–501.
13. Egerer, J., Desel, T., Popken, G., Boxho, J., Macq, D., & Cornil, J. (1998). A low-distortion linear-tunable continuous-time 488 kHz fifth-order Bessel filter. In *Proc. 11th Annual IEEE Int. Conf. ASIC*, pp. 47–50.
14. Kircay, A., & Cam, U. (2006). A novel log-domain first-order multifunction filter. *Etri Journal, 28*(3), 401–404.
15. Kilinc, S., & Cam, U. (2005). Realization of n-th order voltage transfer function using a single operational trans resistance amplifier. *Etri Journal, 27*(5), 647–650.
16. Sagbas, M., & Fidanboylu, K. (2004). Electronically tunable current-mode second-order universal filter using minimum elements. *Electronics Letters, 40*(1), 2–4. doi:10.1049/el:20040013.
17. Kuo, K. C., & Leuciuc, A. (2001). A linear MOS transconductor using source degeneration and adaptive biasing. *IEEE Transactions on Circuits and Systems II-Analog and Digital Signal Processing, 48*(10), 937–943. doi:10.1109/82.974782.

18. Minaei, S., Sayin, O. K., & Kuntman, H. (2006). A new CMOS electronically tunable current conveyor and its application to current-mode filters. *IEEE Transactions on Circuits and Systems I, Regular Papers, 53*(7), 1448–1457. doi:10.1109/TCSI.2006.875184.
19. Ferri, G., & Guerrini, N. (2001). High-valued passive element simulation using low-voltage low-power current conveyors for fully integrated applications. *IEEE Transactions on Circuits and Systems II-Analog and Digital Signal Processing, 48*(4), 405–409. doi:10.1109/82.933805.
20. Wang, H. Y., & Lee, C. T. (2001). Versatile insensitive current-mode universal biquad implementation using current conveyors. *IEEE Transactions on Circuits and Systems II-Analog and Digital Signal Processing, 48*(4), 409–413. doi:10.1109/82.933806.
21. Cicekoglu, O. (2001). Current-mode biquad with a minimum number of passive elements. *IEEE Transactions on Circuits and Systems II-Analog and Digital Signal Processing, 48*(1), 221–222. doi:10.1109/82.917795.
22. Elwan, H. O., & Soliman, A. M. (1996). A novel CMOS current conveyor realization with an electronically tunable current mode filter suitable for VLSI. *IEEE Transactions on Circuits and Systems II-Analog and Digital Signal Processing, 43*(9), 663–670. doi:10.1109/82.536763.
23. Horng, J. W. (2001). High-input impedance voltage universal biquadratic filter using three plus-type CCIIs. *IEEE Transactions on Circuits and Systems II-Analog and Digital Signal Processing, 48*(10), 996–997. doi:10.1109/82.974791.
24. Horng, J. W., Hou, C. L., Chang, C. M., et al. (2006). Quadrature oscillators with grounded capacitors and resistors using FDCCIIS. *Etri Journal, 28*(4), 486–494.
25. Piovaccari, A. (1995). CMOS integrated third-generation current conveyor. *Electronics Letters, 31*(15), 1228–1229. doi:10.1049/el:19950882.
26. Horng, J. W., & Lee, M. H. (1997). High input impedance voltage-mode lowpass, bandpass and highpass filter using current-feedback amplifier. *Electronics Letters, 33*(11), 947–948.
27. Acar, C. (1997). Universal current-mode filter with reduced number of active and passive components. *Electronics Letters, 33*(11), 948–949.
28. Moon, U. K., & Song, B. S. (1993). Design of a low-distortion 22 kHz fifth-order Bessel filter. *IEEE Journal of Solid-State Circuits, 28*(12), 1254–1264. doi:10.1109/4.261999.
29. Yang, F., & Enz, C. C. (1996). A low-distortion BiCMOS seventh-order Bessel filter operating at 2.5 V supply. *IEEE Journal of Solid-State Circuits, 31*(3), 321–330. doi:10.1109/4.494194.
30. Chang, Z. Y., Haspelagh, D., & Vrfaillie, J. (1997). A highly linear CMOS Gm-C bandpass filter with on-chip frequency tuning. *IEEE Journal of Solid-State Circuits, 32*(3), 388–397. doi:10.1109/4.557637.
31. Groenewold, G. (2000). Low-power MOSFET-C 120 MHz Bessel allpass filter with extended tuning range. *IEE Proceedings Circuits, Devices and Systems, 147*(2), 28–34. doi:10.1049/ip-cds:20000045.
32. Schmid, H.·P., & Moschytz, G. S. (2000). Active MOSFET-C single amplifier biquadratic filters for video frequencies. *IEE Proceedings Circuits, Devices and Systems, 147*(2), 35–41. doi:10.1049/ip-cds:20000046.
33. Yamazki, H., Oishi, K., & Gotoh, K. (1999). An accurate center frequency tuning scheme for 450-kHz CMOS Gm-C bandpas filter. *IEEE Journal of Solid-State Circuits, 34*(12), 1691–1697. doi:10.1109/4.808894.
34. Khoury, J. M. (1991). Design of 15-MHz CMOS continuous-time filter with on-chip tuning. *IEEE Journal of Solid-State Circuits, 26*(12), 1988–1997. doi:10.1109/4.104193.
35. Osa, J. I., Carlosena, A., & Lopez-Martin, A. J. (2001). MOSFET-C filter with on-chip tuning and wide programming range. *IEEE Journal of Solid-State Circuits, 48*(10), 944–951.
36. Silva-Martinez, J., Steyaert, M., & Sansen, W. (1992). A 10.7 MHz 68-dB SNR CMOS continuous-time filter with on chip tuning. *IEEE Journal of Solid-State Circuits, 27*(12), 1843–1852. doi:10.1109/4.173114.
37. Chang, Z. Y., Macq, D., Haspeslagh, D., et al. (1995). A CMOS analog front-end circuit for an FDM-based ADSL system. *IEEE Journal of Solid-State Circuits, 30*(12), 1449–1456. doi:10.1109/4.482192.
38. Hollman, T., Lindfors, S., et al. (2001). A 2.7-V CMOS dual-mode baseband filter for PDC and WCDMA. *IEEE Journal of Solid-State Circuits, 36*(7), 1148–1153. doi:10.1109/4.933475.
39. Tsividis, Y., & Banu, M. (1986). Continuous-time MOSFET-C filters in VLSI. *IEEE Journal of Solid-State Circuits, SC-21*(1), 15–30. doi:10.1109/JSSC.1986.1052478.
40. He, Y., Jiang, J., & Sun, Y. (2002). CMOS R-MOSFET-C fourth-order Bessel filter with accurate group delay. In *Proc. IEEE ISCAS* (Vol. 4, pp. 245–248). Arizona, USA.
41. Fiez, T., & Allstot, D. (1990). CMOS switched-current ladder filters. *IEEE Journal of Solid-State Circuits, 25*(6), 1360–1367. doi:10.1109/4.62163.
42. Baruqui, F. A. P., & Petraglia, A. (2006). Linearly tunable CMOS OTA with constant dynamic range using source-degenerated current mirrors. *IEEE Transactions on Circuits and Systems II. Express Briefs, 53*(9), 797–801. doi:10.1109/TCSII.2006.881162.
43. Chatterjee, S., Tsividis, Y., & Kinget, P. (2005). 0.5-V analog circuit techniques and their application in OTA and filter design. *IEEE Journal of Solid-State Circuits, 40*(12), 2373–2387. doi:10.1109/JSSC.2005.856280.

Jinguang Jiang received the Bachelor degree and MSc degree from Hunan University, Hunan, China, in 1993, 1998 and the PhD degree from Hunan University, China, in 2003, all in Electrical Engineering. From June 2004 to June 2006, He was a Post-doctoral fellow of Control Science and Engineering in the Faculty of Electrical and Information Engineering at Hunan University. He is currently a Professor of GNSS Research Center, Wuhan University. His research interests are high performances Digital to Analog Converter, Filter and RF integrated circuits, low voltage, low power Mixed-Signal integrated circuits design, etc.

Yigang He received the MSc degree from Hunan University, Hunan, China, in 1992 and the PhD degree from the University of Xi'an Jiaotong, China, in 1996, all in Electrical Engineering. He is currently a Professor of Electrical Engineering in the Faculty of Electrical and Information Engineering at the University of Hunan. He was a Senior Visiting Scholar at the University of Hertfordshire, UK, in 2002. His research interests are in analog

and Mixed-Signal circuits, fault diagnosis and testing, and signal processing; RF and communication circuits; and wireless and mobile communication systems. He has published some 180 journal and conference papers in these areas. He has been on the Technical Programme Committees of a number of international conferences. He is a Member of IEE and IET, and has obtained a number of national awards, prizes, and honors.